Journal of Materials Chemistry A

Polymer Aggregation Control in Polymer:Fullerene Bulk Heterojunctions Adapted from Solution

Journal:	*Journal of Materials Chemistry A*
Manuscript ID:	TA-ART-09-2014-004736.R1
Article Type:	Paper
Date Submitted by the Author:	20-Oct-2014
Complete List of Authors:	Kästner, Christian; Technische Universität Ilmenau, Institute of Physics Egbe, Daniel; Johannes Kepler University Linz, Austria, Linz Institute of Organic Solar Cells Hoppe, Harald; Technische Universität Ilmenau, Institute of Physics

Polymer Aggregation Control in Polymer:Fullerene Bulk Heterojunctions Adapted from Solution

Christian Kästner[1], Daniel A. M. Egbe[2], Harald Hoppe[1]

[1] Institute of Physics, Ilmenau University of Technology, Langewiesener Str. 22, 98693 Ilmenau, Germany

[2] Linz Institute for Organic Solar Cells, Johannes Kepler University Linz, Altenbergerstr. 69, 4040 Linz, Austria

Abstract: It is common knowledge that the polymer conformation and its phase separation with fullerene derivatives are delicate issues crucially impacting on the photovoltaic parameters of polymer based solar cells. Whereas strongly intermixed polymer:fullerene phases presumably provide large interfacial area and consequently a high quantum efficiency of exciton dissociation, pristine and primarily ordered polymer and fullerene domains may support efficient charge transport and its percolation. To study the aggregation and phase separation behaviour in polymer solar cells we investigated counterbalancing influences of polymer solution concentration and its blending ratio with PCBM ([6,6]-phenyl-C61-butyric acid methyl ester) on the basis of a semi-crystalline anthracene-containing poly(*p*-phenylene-ethynylene)-*alt*-poly(*p*-phenylene-vinylene) (PPE-PPV) copolymer statistically bearing branched 2-ethylhexyloxy and linear octyloxy side-chains (AnE-PV*stat*). The polymer aggregation was semi-quantitatively evaluated on the basis of its optical fingerprints and varied with both, the solution and the PCBM concentration, yielding a specific maximum within the parameter range studied. Upon relating photovoltaic parameters with the order within the polymer phase, the counterbalancing effect between charge generation and transport for increasing polymer aggregation is demonstrated, in agreement with sound hypotheses.

Introduction

The continuously increasing research interest in polymer-based organic photovoltaics (polymer solar cells) over the last two decades,[1,2,3,4] resulted in improved fundamental and technological knowledge concerning polymer solar cells as a flexible[5,6,7] and semi-transparent[8,9,10] option for harvesting solar radiation at potentially low cost.[11,12,13] But there are still big efforts to be undertaken in order to match the requirements of future power installations similar to conventional, inorganic photovoltaics. In

general highly efficient polymer solar cells are based on the bulk heterojunction (BHJ)[14,15] concept – in which the intimate intermixing of electron donating polymers and electron acceptors provides an efficient ultra-fast charge transfer within this blend.[16,17,18] Among the most suited acceptors for efficient bulk heterojunction solar cells are fullerene derivatives, most commonly PCBM.[18,19]

Since charge separation of excitons takes place at the interface between polymer and PCBM, an intimate mixture of both materials is successful for splitting the photogenerated excitons due to the large interfacial area, yielding high charge generation rates.[16,17,20] In contrast,, recombination rates are also increased as charge percolation is limited within homogeneously intermixed phases yielding to losses in photocurrent.[21] Hence a pristine polymer phase may reduce charge recombination, while the hole mobility is additionally controlled by the order within the polymer phase[21,22,23,24] - π–π-stacking on the short-range and crystallinity on the long-range order[25,26,27,28] as well as by phase purity.[29] The electron transport capability is comparably high within the PCBM phase, already benefitting from higher order easily obtained in aggregates of spherical fullerene derivatives.[30,31] Furthermore, fullerene aggregation/crystallization promotes the charge separation within bulk heterojunctions due to the multitude of energy levels present for charge transfer.[20,32,33] Thus, large phase separation between polymer and PCBM improves the charge extraction from the bulk, but leads to a loss of interfacial area and thus potentially photocurrent. Contrarily, a strong intermixing leads to large interfacial area and thus charge generation, but a loss in charge percolation pathways and thus to increased charge recombination. Furthermore, excitons generated within pristine bulk material have to reach the interface between polymer and PCBM for dissociation. But, the limited exciton life-time and consequently its diffusion length of approximately 10 - 20 nm require pristine domain sizes of limited size, which still allow excitons to reach the interface.[34,35] Conclusively, charge generation, recombination and percolation counterbalance each other and they are controlled by the morphology of the bulk heterojunction.[36,37,38,39] Thus, a fine-tuned blend morphology is required to maximize charge generation and minimize charge recombination due to improved charge transport and extraction.

Several approaches were pursued to control the nanomorphology of organic bulk heterojunctions. For example, the so-called micro-phase separation between donor and acceptor could be obtained by utilization of block copolymers consisting of alternating well-aligned donor and acceptor blocks fulfilling the requirements of suitable phase separation.[40,41] In case of binary donor-acceptor systems, like the well-known semi-crystalline poly(3-hexylthiophene) (P3HT), post-production treatments such as thermal annealing[42,43] or slow drying[44] improved the solar cell performance by enhanced structural ordering, respectively the controlled crystallization of P3HT.[45] Several approaches for controlling the P3HT aggregation already within solution were pursued in order to yield an improved morphology control for the evolving bulk heterojunction.[46,47,48,49,50] The formation of semi-crystalline P3HT fibres

was for example achieved by aggregation induced by use of non-solvents as additives within the P3HT-solution.[49,51] Amorphous polymer based systems could be improved by increased phase separation between PCBM and an intercalated polymer:PCBM mix-phase[52] utilizing solvent blends or additives[53,54,55]. However, those systems still lack performance due to the amorphous nature of the polymer and limited hole percolation.[22,56,57,58]

In this work we present an approach to precisely control structural order of the polymer as well as phase separation between polymer and PCBM. The herein used copolymer AnE-PV*stat* is semi-crystalline as obtained from wide-angle x-ray scattering experiments.[25] Previous studies revealed the degree of aggregation of semi-crystalline AnE-PV to be improved by the presence of PCBM.[59,60] Furthermore, the degree of phase separation between AnE-PV copolymers and PCBM can be controlled by the solvent composition of chloroform and chlorobenzene and the PCBM concentration within the common solution. An optimized phase separation of AnE-PV copolymers with PCBM was obtained for a 1:1 ratio of chloroform and chlorobenzene based solutions.[61] Based on its ability to aggregate and phase separate with PCBM, AnE-PV*stat* constitutes a perfect candidate to study the influence of structural order and phase separation on the solar cell device operation. In the following, the blend morphology was precisely controlled by solution concentration and PCBM weight fraction. The quantification of polymeric structural order in this material system is achieved by the introduction of a parameter of combined structural order, derived from the relative changes in inter-chain and intra-chain order of polymer aggregates, probed with optical steady-state spectroscopy.

Theoretical Background

The analytical model used in our studies for quantifying polymeric order is based on the assumptions for H- and J-aggregation of polymers as proposed by Spano et al., whereas absorption spectroscopy generally reveals information about inter-chain order and photoluminescence spectroscopy about intra-chain order, compare with Figure 1.[62,63,64] The optical absorption and emission of J-aggregates, described by the HJ-aggregate model, is explicitly linked with the polymeric order: the ratio of the 0-0 to 0-1 transition of the absorption spectrum, $A_{0\text{-}0}/A_{0\text{-}1}$, increases with increasing order as well as the ratio of the polymer photoluminescence emission $E_{0\text{-}0}/E_{0\text{-}1}$ at room temperature.[63] Apart from that, it is also well known that the near-field order, generated by the π–π–stacking of the polymer backbones, is parental for the origination of the 0-0 peak transition in the polymer absorption spectra.[65,66] Furthermore, the absorption spectra also contain information about the degree of conjugation.[67,68] J-aggregation has extensive consequences on the electrical properties: the intra-chain coupling is much stronger than the inter-chain coupling and leads therefore to large free charge carrier mobilities,[69] but comparable low exciton mobilities along the polymer backbone.[70]

To globally define the polymer order within the system, we linked the inter-chain order, represented by π–π–stacking of polymer backbones, to the intra-chain order, represented by torsion-free planarization of polymer backbones. Hence the product of the $A_{0\text{-}0}/A_{0\text{-}1}$ polymer absorption peak ratio and the $E_{0\text{-}0}/E_{0\text{-}1}$ polymer emission peak ratio can be defined as the parameter of combined structural order, P_{CSO}, valid for J-aggregates and under the assumption that inter- and intra-chain order must be strongly correlated. As within aggregates both conditions, intra-chain and inter-chain order, have to be fulfilled, the combined structural order parameter is introduced as product of both individual order parameters. An arithmetic average, i.e. the weighted sum of both parameters, constitutes a weaker and compromising condition and is therefore discarded.

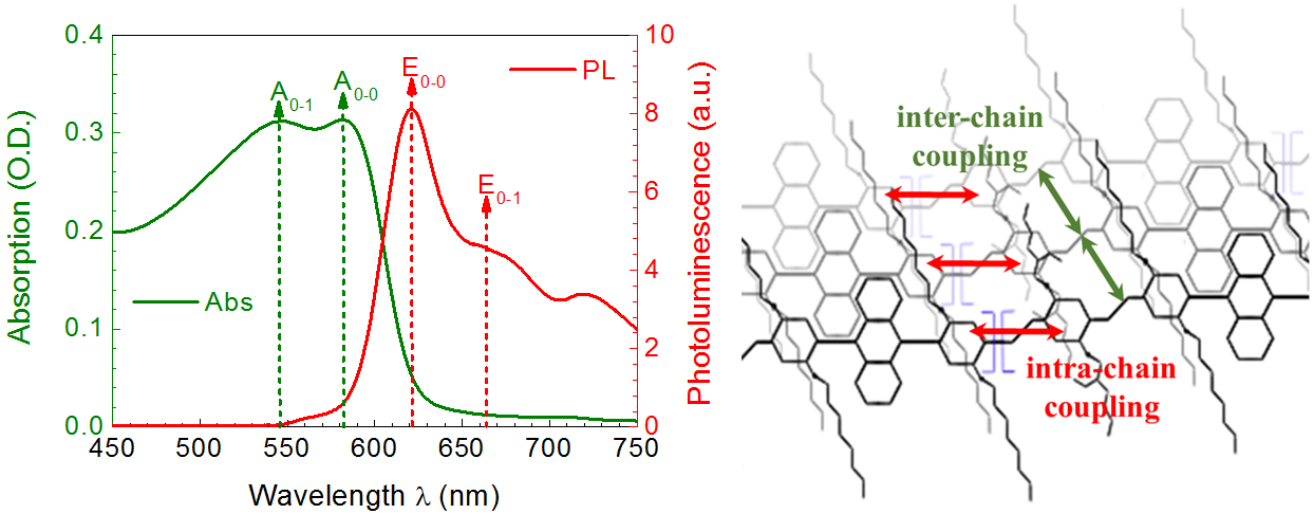

Figure 1: Correlation between emission/absorption transitions, $E_{0\text{-}0}/E_{0\text{-}1}$ and $A_{0\text{-}0}/A_{0\text{-}1}$, and intra-chain/inter-chain coupling for J-aggregated AnE-PV.

Next to the intra-chain order of polymer backbones, photoluminescence spectroscopy allows semi-quantitative insights into the degree of phase separation between polymer and PCBM.[71] Usually, the degree of polymer aggregation is accompanying the degree of phase separation between polymer and PCBM due to the fact that the undisturbed pristine polymer phase is more prone to reorganize within an ordered structure by free energy minimization.[72] We have already shown that semi-crystalline AnE-PV tends to phase separate strongly from PCBM.[60] An earlier comparison between the domain size and photoluminescence yield of thin AnE-PV:PCBM blend films yielded good agreement with x-ray diffraction results.[73] Whilst strongly phase separated systems showed remaining photoluminescence from both materials, strong intermixing led to substantial quenching of the polymer photoluminescence signal, and to the occurrence of interfacial charge transfer photoluminescence (CT-PL) signals.[60,74] Thus photoluminescence provides potentially a lot of information about the scale of phase separation within bulk heterojunction blends.

Experimental

Scheme 1 displays the chemical structures of AnE-PV*stat* and PCBM, which were used within this study. AnE-PV*stat* was synthesized as reported earlier.[59] As electron acceptor, PCBM was used as obtained from the supplier (Nano-C, USA).

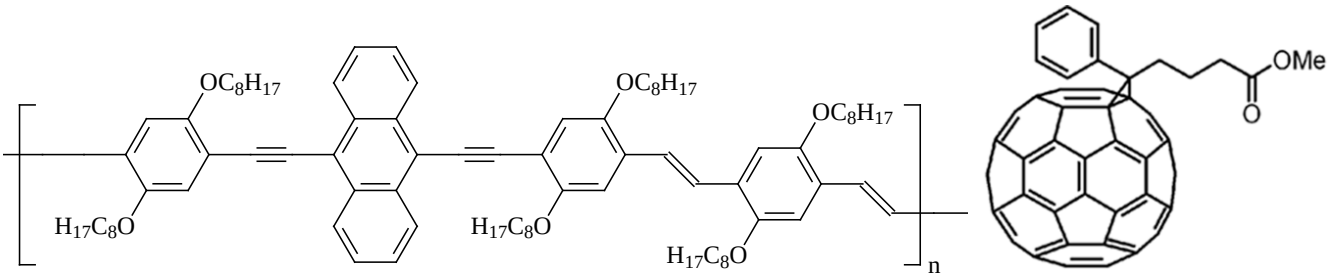

Scheme 1: Molecular structure of AnE-PV*stat* (C_8H_{17} = octyl and/or 2-ethylhexyl) and PCBM.

Thin films of AnE-PV*stat*:PCBM blends were spin cast onto glass substrates using 1:1 mixtures of chloroform:chlorobenzene based solutions under nitrogen atmosphere. Thin film absorption spectra were recorded with a Varian Cary 5000 UV/Vis spectrophotometer under 2-beam VW-setup condition to determine the sample absorption via transmission and reflection measurements. Thin film photoluminescence (PL) spectra were recorded with an Avantes avaspec 2048 fiber spectrometer within a range from 500 to 1100 nm and were normalized to the film absorption at the laser excitation wavelength of 445 nm. All optical characterizations were executed at room temperature.

Solar cell device preparation on glass involved partly etching of the ITO-layer for selectively contacting of the back electrode, followed by spin coating of PEDOT:PSS (Clevios PH, Heraeus). The PEDOT:PSS layers were annealed at 170°C for 15 minutes to release water moieties and were afterwards transferred to a nitrogen (N_2) glovebox for further processing of photoactive layers. The photoactive layers were spin cast from AnE-PV*stat*:PCBM solutions with blend ratios varying from 1:1 to 1:2 by weight (polymer:fullerene) and a solution concentration varying from 0.4 to 0.6 wt.-% of the polymer part. Spin frequencies were varied from 500 to 1600 rpm to evaluate the optimum layer thickness for every blend. The top aluminum electrode was deposited by physical vapor deposition. Current-voltage (IV) measurements of solar cell devices exhibiting an active area of 0.5 cm^2 were recorded with a Keithley 2400 Source-Measure-Unit using a class A solar simulator. The external quantum efficiency spectra were recorded using bias illumination to resemble current densities typical under one sun illumination. Neither thin films prepared for the optical investigations nor those prepared for solar cell devices were annealed.

Results and Discussion

To elucidate the influence of solution concentration and AnE-PV*stat*:PCBM blend ratio on the π–π stacking of AnE-PV*stat*, absorption spectra of thin films were recorded. Figure 2 depicts the thin film absorption spectra of AnE-PV*stat* blended with different amount of PCBM at various solution concentrations. Spectra were normalized to the 0-1 transition peak height to highlight the relative change with respect the 0-0 transition. Figure 2 a), b) and c) show the absorption of the AnE-PV*stat*:PCBM blend films over the full measurement range and d) depicts the zoom-in spectrum, spanning over the absorption edge with the 0-0 and 0-1 transition to highlight the degree of π–π–stacking induced order.

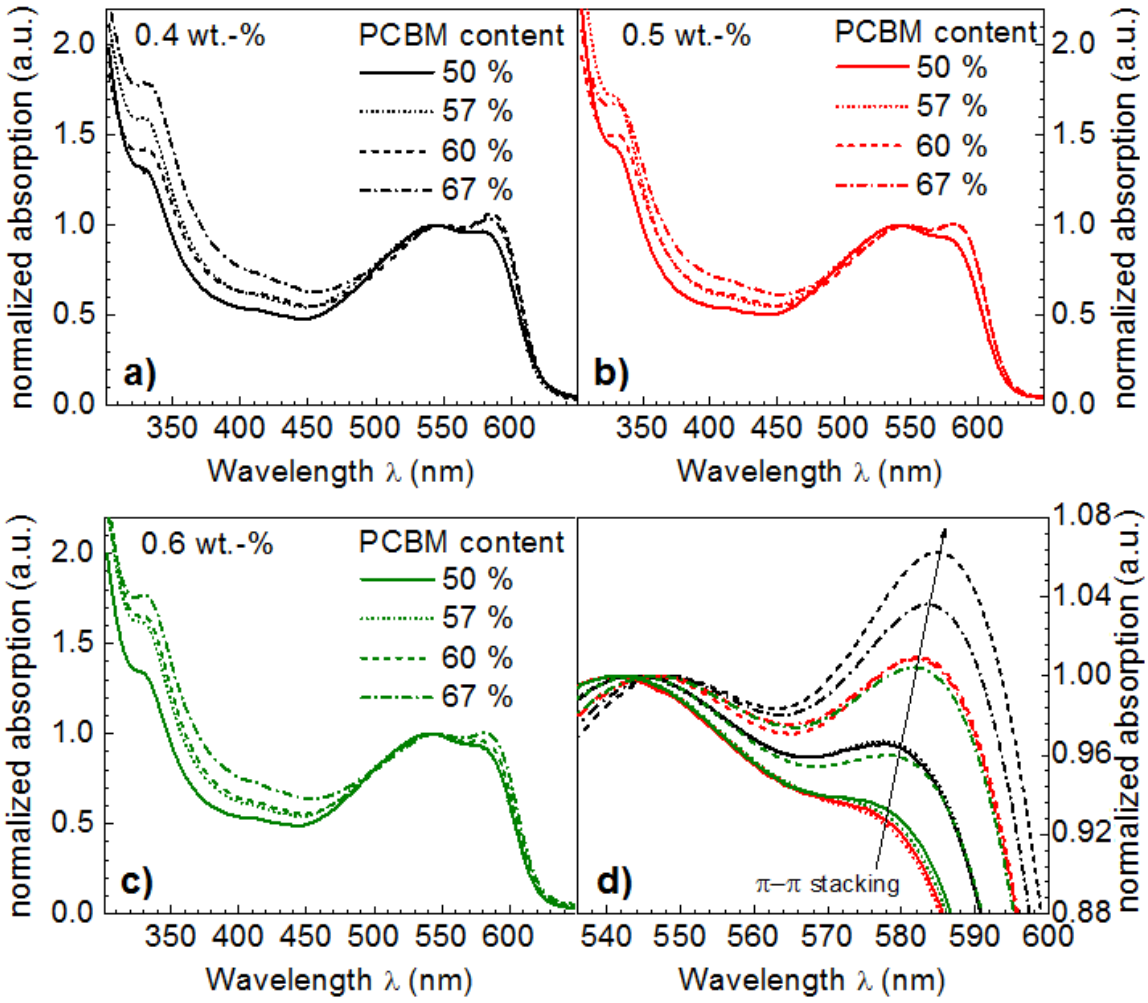

Figure 2: Thin film absorption spectra of AnE-PV*stat*:PCBM films, normalized to the 0-1 transition at around 545 nm to highlight the evolution of the 0-0 transition at around 585 nm, as function of the AnE-PV*stat* solution concentration and the PCBM weight fraction. Full spectra are shown in a), b) and c); zoom-in spectra, highlighting the occurrence of the AnE-PV*stat* π–π-stacking, are shown in figure d).

The polymer-fullerene blend ratio and the polymer solution concentration imposed a strong impact on the aggregation behavior of AnE-PV*stat* which was related to the red-shift of the polymer absorption accompanied by the typical 0-0 transition at the absorption edge of the polymer. The reduced probability for the entanglement of polymers within diluted solutions seems to promote the formation of aggregates. Hence the larger degree of freedom enables aggregation, whereas higher solution concentrations may hinder the aggregate formation due to entanglement. Generally, the peak height of the 0-0 transition and thus the order increased with increasing amount of PCBM at a certain solution concentration as well as with decreasing solution concentration at a certain AnE-PV*stat*:PCBM blend ratio. The induced polymer aggregation upon addition of PCBM was already discovered earlier for the semi-crystalline analogue AnE-PV*ab*.[59,60] It has been demonstrated that upon blending with PCBM the polymer aggregation generally increased. However, the maximum polymer aggregation was not found for largest PCBM concentration at lowest solution concentration, but instead for a AnE-PV*stat*:PCBM blending ratio of 2:3 for 0.4 wt.-% solution concentration of AnE-PV*stat*. This can be understood as with further increasing the PCBM content the diffusion rate of PCBM into the polymer domains grows by the progressive concentration gradient. In contrast to PBTTT, the PCBM does not form interdigitated nano-crystallites with AnE-PV*stat*.[76,77,78] Thus higher volume fractions and thus concentrations of incorporated PCBM molecules tended to distort the polymeric order, which resulted in a slight reduction of the 0-0 transition oscillator strength. In conclusion, both parameters, PCBM volume fraction and polymer solution concentration, may counterbalance the degree of polymer aggregation and presumably the pristine domain sizes.

For a semi-quantitative analysis, the ratio between 0-0 peak and 0-1 peak heights was taken as a measure for the degree of polymer aggregation.[62,63,64] To visualize the degree of polymer aggregation – appointed to the π–π–stacking of AnE-PV*stat* – the normalized peak height ratios are plotted as function of the processing parameters AnE-PV*stat* concentration and AnE-PV*stat*:PCBM blend ratio in Figure 5 a). It should be noted that even lower solution concentrations might lead to stronger polymer aggregation, as the observed maximum of the polymer aggregation is located at the edge of the investigated range. However, too low solution concentrations led to processing difficulties i.e. unacceptable film homogeneities, so that the required active layer thicknesses for solar cell application were not obtained any more. Thus, lower solution concentrations than 0.4 wt.-% were irrelevant and not further be considered.

To elucidate the influence of solution concentration and AnE-PV*stat*:PCBM blend ratio on backbone planarization of AnE-PV*stat*, photoluminescence spectra of the identical thin films were recorded. Figure 3 depicts the obtained thin film photoluminescence spectra of AnE-PV*stat* blended with different amounts of PCBM at various solution concentrations. Figure 3 a), b) and c) show the fully

recorded wavelength range photoluminescence spectra of the AnE-PV*stat*:PCBM blend thin films whilst d) shows the photoluminescence normalized to the 0-0 emission of the polymer within a zoom-in range, highlighting the typical photoluminescence contributions of AnE-PV*stat* and PCBM.

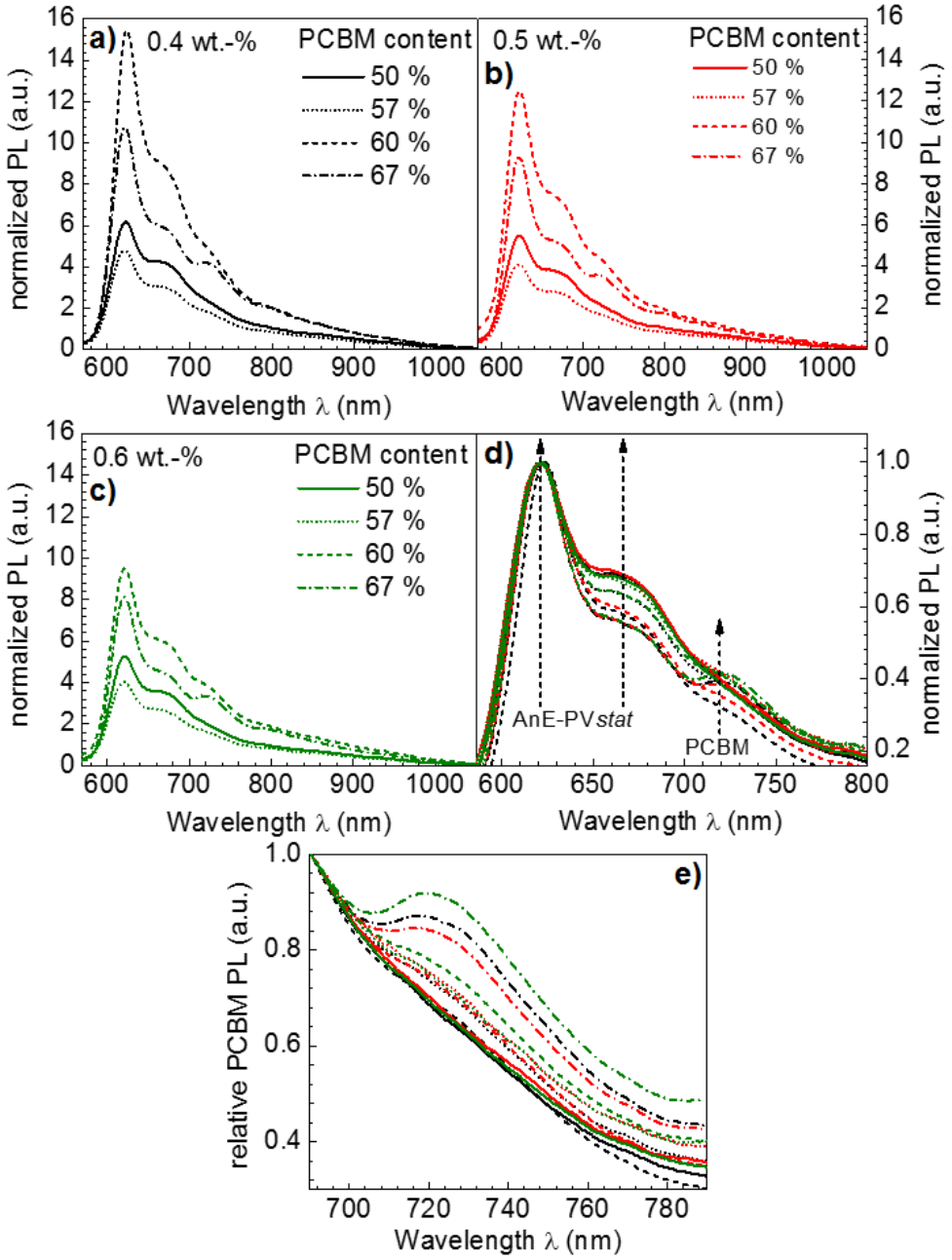

Figure 3: Thin film photoluminescence spectra of AnE-PV*stat*:PCBM films normalized to the thin film absorption at the 445 nm laser excitation wavelength as function of the AnE-PV*stat* solution concentration and the PCBM weight fraction. Full range PL-spectra are shown in a), b) and c); the to the 0-0 transition normalized zoom-in spectra of all samples, enabling a comparison concerning aggregation of AnE-PV*stat* and domain size evolution of PCBM, are shown in d). The evolution of the relative PCBM PL peak strengths (for highlighting, spectra are normalized to the PL at 690 nm) are depicted in e).

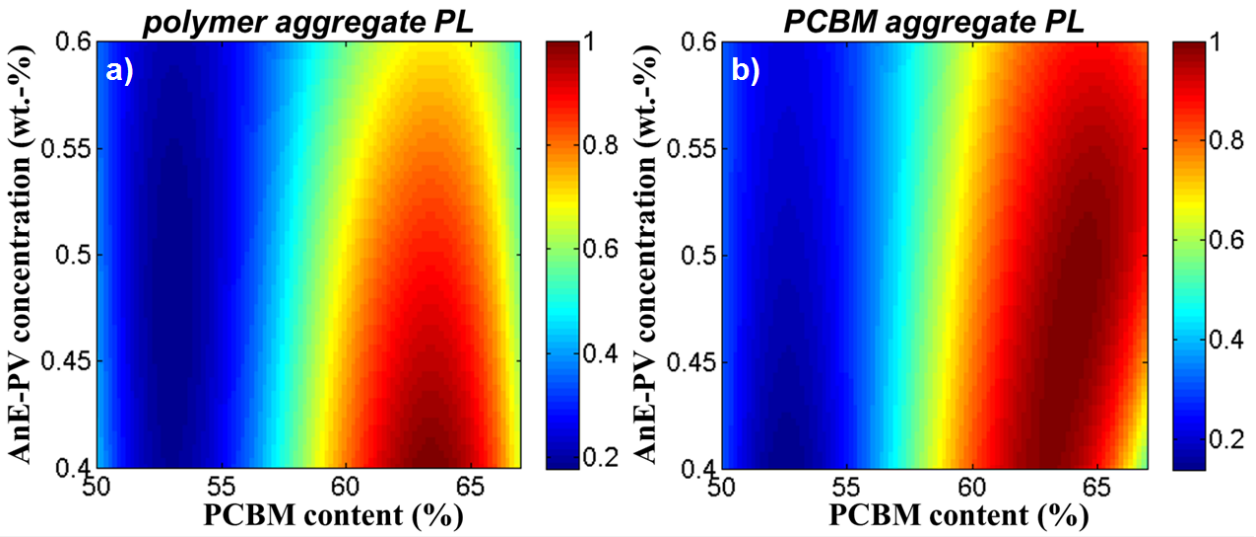

Figure 4: Interpolated contour plots of the photoluminescence intensity of a) polymer and b) PCBM as function of processing parameters.

The overall polymer photoluminescence signal strength (Figure 4 a) is directly correlated to the volume of pristine polymer phases in the film, in which the excitons are not able to reach an interface with PCBM during their lifetime. As the PL-signal intensity varied much more strongly over the entire processing parameter range than the increase of the volume fraction of ordered polymer phases, which is estimated by the relative increase in inter-chain order (compare with Figure 4 a), it is indicated that the domain size is varied 3-dimensionally. For PCBM a similarly large variation in PL-signal intensity was found and larger PCBM domains are conclusively found for largest PCBM concentrations (i.e. 1:2 AnE-PV*stat*:PCBM blend ratios).[79]

Overall the maximum polymer PL signal – involving largest polymer domain size – is observed for 0.4 wt.-% AnE-PV*stat* solution concentration and a 2:3 blending ratio of AnE-PV*stat*:PCBM. This is in accordance to the observations from the absorption measurements – the maximum polymer aggregation was found for the same concentration and blend ratio.

Figure 5 summarizes the normalized parameters for inter- and intra-chain order. The strongest influence on both order parameters is imposed by the PCBM concentration, whereas the polymer solution concentration showed a stronger influence on the inter-chain as compared to the intra-chain order. For further considerations and as a compromise, the two order parameters were unified into a single combined structural order parameter, P_{CSO}, as defined above (Figure 5 c).

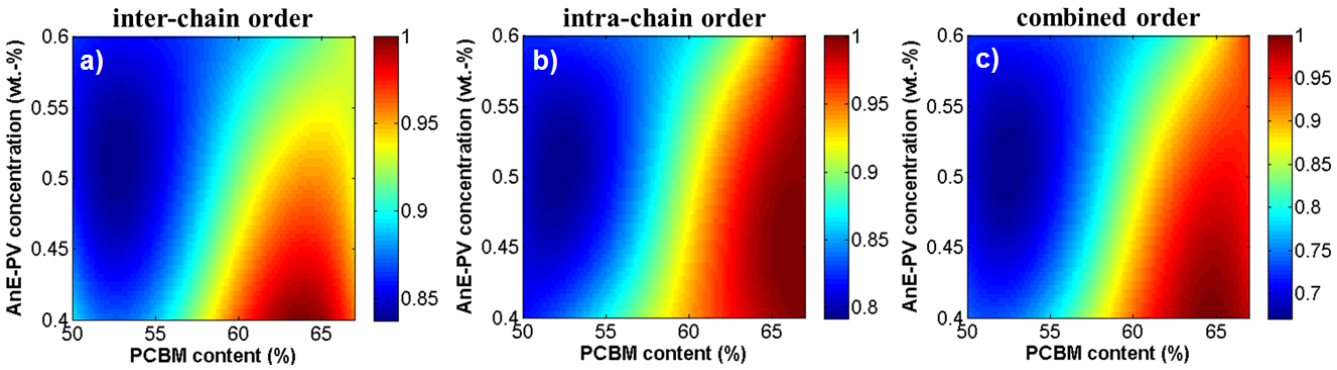

Figure 5: Interpolated contour plots of the a) $A_{0\text{-}0}/A_{0\text{-}1}$ ratio of the polymer transition peak heights from absorption as a measure for inter-chain order, (compare with Figure 2), and of the b) $E_{0\text{-}0}/E_{0\text{-}1}$ polymer emission peak ratio obtained from photoluminescence as a measure for intra-chain order (compare with Figure 3 d), and c) of the product of both order parameters as a measure for combined structural order (P_{CSO}) as function of the AnE-PV*stat* solution concentration and the PCBM weight fraction.

In summary, the optical characterization revealed that AnE-PV*stat* forms J-aggregates, since for absorption and photoluminescence the 0-0 peak could raise above the 0-1 peak. Coupling the intra-chain order and inter-chain order to a common parameter of combined structural order allowed to quantify the general degree of order in polymer aggregates. Finally, both the polymer order and the blend phase separation were controlled by solution concentration and dominantly by the PCBM content.

To gain additional insight into the blend film morphology atomic force microscopy (AFM) measurements were carried out in tapping mode. All obtained topography images of 2.5 µm × 2.5 µm scans of the blend films are shown in Figure 6. At lower PCBM contents a fine-scale structure is observed. With increasing PCBM content larger domains evolve, presumably originating from increasing PCBM inclusions.[71] On top of these fullerene aggregates polymer aggregates of AnE-PV*stat* are clearly visible. In good agreement with the photoluminescence data, the PCBM aggregates increased with increasing PCBM concentration and lowered polymer solution concentration, which is also reflected in the surface roughness contour plot in Figure 7. Thus the pronounced self-aggregation of AnE-PV*stat* in more diluted solutions seems to support the evolution of larger PCBM domains.

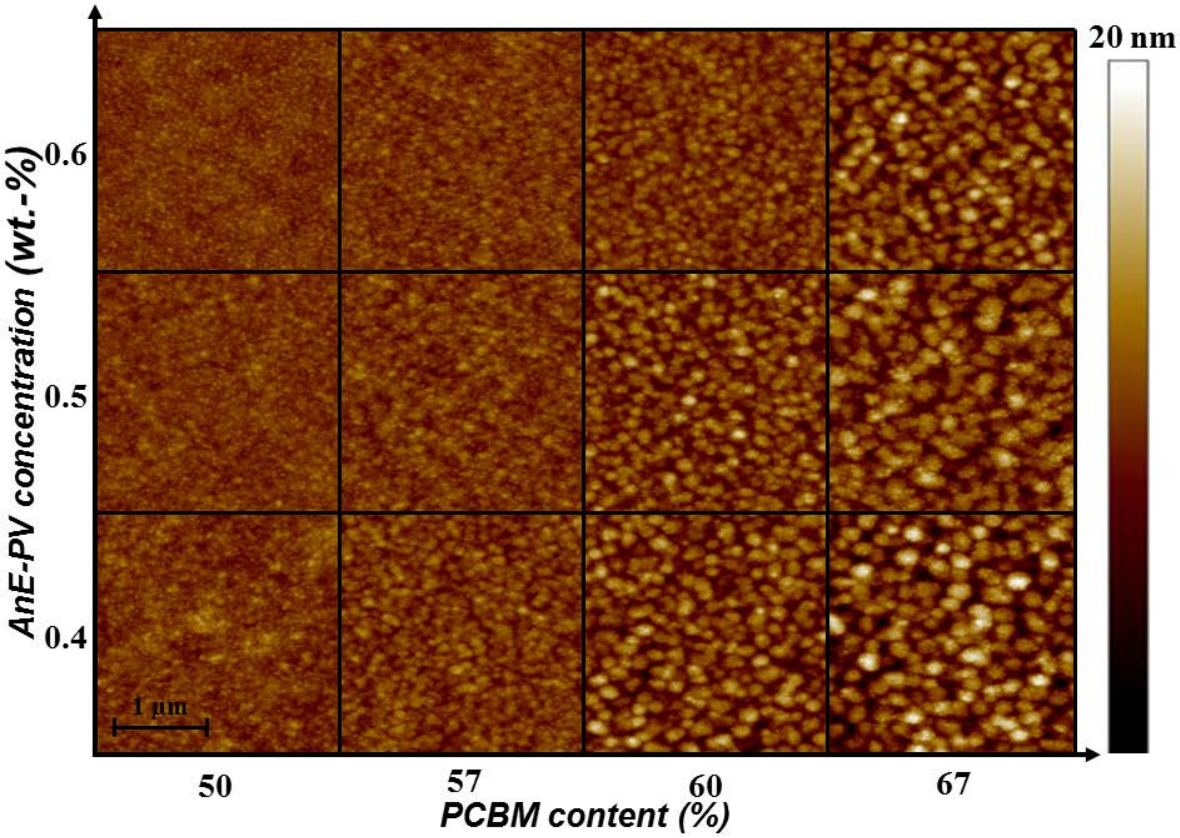

Figure 6: Tapping mode 2.5 µm × 2.5 µm topography images (20 nm height scale) of AnE-PV*stat*:PCBM blend thin films as function of AnE-PV*stat* solution concentration and PCBM content.

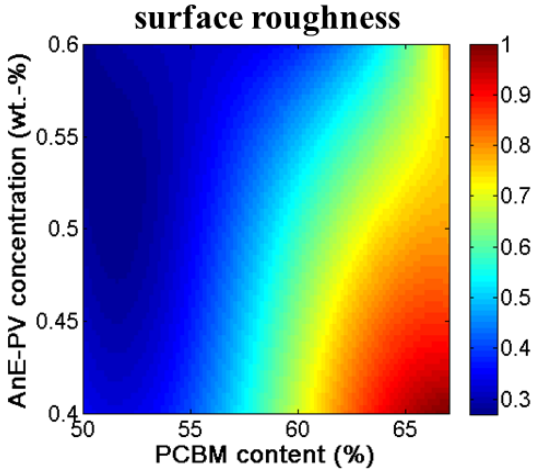

Figure 7: Normalized mean-square surface roughness, taken from AFM images, as function of PCBM content and AnE-PV solution concentration. For visualization, the data points were entered into a matrix that was zero-filled and linearly interpolated between the experimental data points.

To gain insight into the influence of polymer aggregation and phase separation between AnE-PV*stat* and PCBM on the opto-electronic properties of bulk heterojunctions, solar cells were fabricated, spanning over the same range of processing parameters, and characterized. The current-voltage (J-V)

characteristics and EQE spectra of all photovoltaic devices are shown in Figure 8. Indeed, the EQE spectra confirmed the short-circuit currents obtained from J-V characteristics. Table 1 depicts the photovoltaic parameters of these solar cells with optimized film thickness.

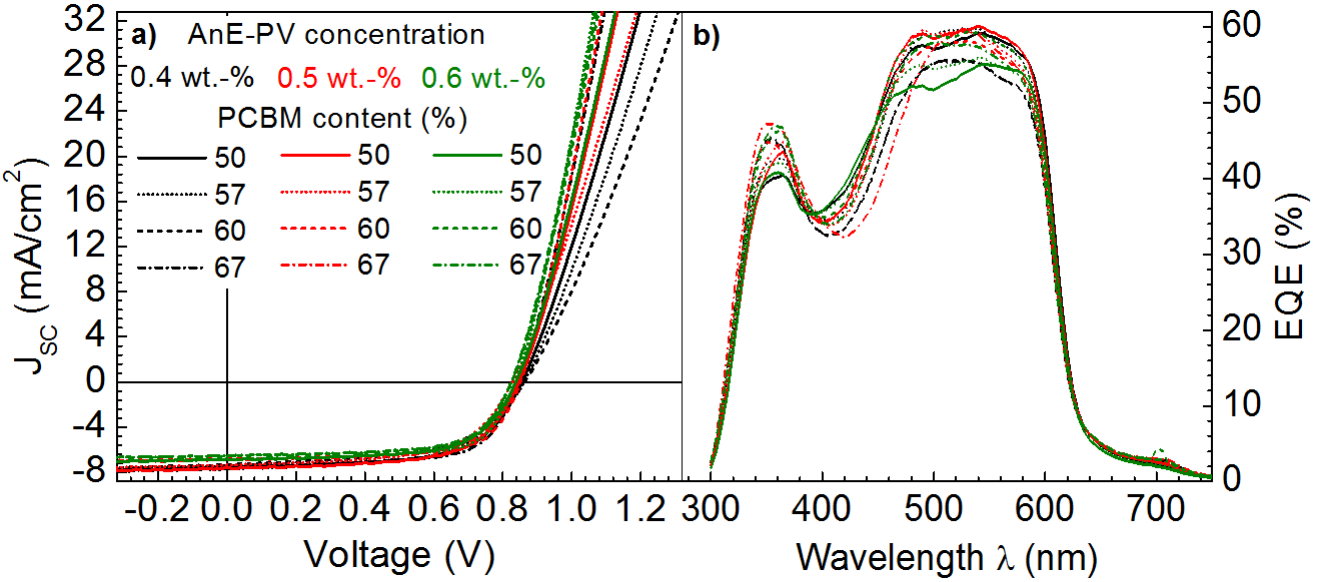

Figure 8: a) Current-voltage characteristics under one sun illumination intensity of film thickness optimized solar cells for different polymer solution concentrations and PCBM weight fractions and b) the corresponding EQE spectra recorded under one sun bias light illumination.

Table 1: Photovoltaic parameters of optimized solar cells fabricated from various AnE-PV*stat*:PCBM solutions defined by the parameter space of different polymer solution concentrations and PCBM weight fractions are summarized. PCE was corrected by integrated photocurrents from measured EQE spectra.

concentration (wt.-%)	*PCBM content (%)*	J_{SC} *(mA/cm²)*	V_{OC} *(mV)*	*FF (%)*	*PCE (%)*	R_S *(Ω)*	R_P *(kΩ)*
0.4	50	7.57	853	63.1	4.07	13.1	2.1
	57	7.52	843	68.2	4.33	10.1	3.0
	60	7.03	848	69.8	4.16	9.5	4.8
	67	7.05	834	68.8	4.04	9.4	2.5
0.5	50	7.62	858	59.7	3.91	14.2	2.3
	57	7.48	842	62.9	3.96	11.5	2.1
	60	7.38	838	66.0	4.08	12.0	3.2
	67	7.18	821	67.0	3.95	10.4	3.7
0.6	50	7.17	861	56.9	3.52	14.9	2.1
	57	7.27	825	60.7	3.64	14.7	2.3
	60	7.61	835	64.4	4.09	11.7	5.8
	67	7.36	820	66.6	4.02	10.3	2.4

The first general observation is that the variation in all photovoltaic parameters remained relatively small and power conversion efficiencies varied around 4%, typical for AnE-PV*stat*.[80] The first conclusion therefore may be, that upon small perturbations of the beforehand optimized donor-acceptor system only gradual changes within the bulk heterojunction blend morphology occurred. In order to visualize the variation in PV-parameters with respect to the processing parameters, the data was interpolated and plotted as function of AnE-PV*stat* solution concentration and AnE-PV*stat*:PCBM blending ratio (Figure 9). At first glance it is obvious that the dependence of many PV-parameters is stronger on the PCBM concentration, respectively the blend ratio, than on the polymer solution concentration. This is especially valid for the short-circuit current density (J_{SC}) and the parallel resistance (R_P) and less strong for the open circuit voltage (V_{OC}). Overall the dependence of fill factor (*FF*) on processing parameters is the most reminiscing of the development of the polymer order as displayed in Figure 3 and Figure 5 above.

For better comparison of the photovoltaic parameters with the underlying polymeric order, the data was replotted with respect to just one parameter of combined structural order (P_{CSO}). The resulting plots are depicted in Figure 10. The graphs show the mean-values with standard deviations as obtained from all solar cells (black squares with error bars) and the corresponding linear fits (red lines) with respect to the P_{CSO}. Indeed the fill factor is most strongly and positively correlated with order of the polymer. Vitarisi et al. found same result for small molecule based organic solar cells: the fill factor increased with degree of phase separation accompanying pristine phase order, indicating reduced recombination losses.[81] Similarly the bulk resistance, expressed by the series resistance (R_S), shows a strong anti-correlation with the increasing order of the polymer. Both parameters thus show that improved polymeric order yields improved charge extraction properties, which are generally provided by an increased mobility-lifetime product. On the other hand, the short circuit photocurrent J_{SC} exhibits an anti-correlation with the polymeric order, which is in agreement with polymer domain coarsening yielding a reduction in the interfacial area between polymer and fullerene derivative. This decrease in photocurrent is furthermore in good agreement with the observed increase in polymer photoluminescence, as depicted in Figure 3 and 4. The open-circuit voltage is slightly anti-correlated with the combined structural order parameter, which is in good agreement with the lowering of the polymer band-gap due to ordering.[20,32,33] Independent of the device film thickness, the highest values of the open-circuit voltage were found for less aggregated, more disordered polymer phases. On the other hand, the less ordered regions of both materials, polymer and PCBM, yield a lower effective HOMO of the polymer[82,83] and a higher effective LUMO of PCBM[33], altogether yielding larger open-circuit voltages.

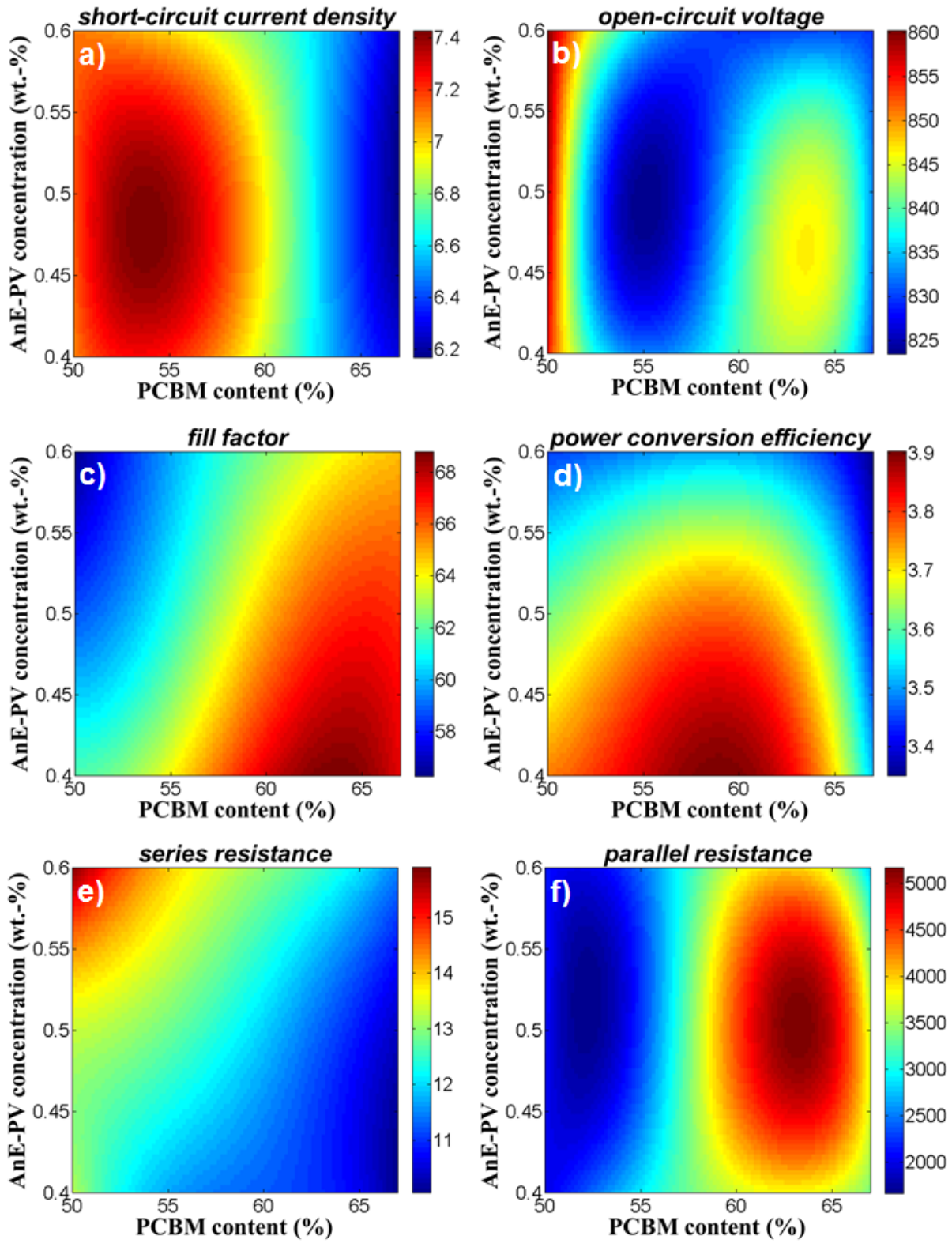

Figure 9: Contour plots of the determined mean-values of all PV-parameters of AnE-PV*stat*:PCBM based BHJ solar cells as function of the AnE-PV*stat* solution concentration and the PCBM weight fraction: a) *short-circuit current density* J_{SC} *(mA/cm²),* b) *open-circuit voltage* V_{OC} *(mV),* c) *fill factor FF (%),* d) *power conversion efficiency PCE (%),* e) *series resistance* R_S *(Ω) and* f) *parallel resistance* R_P *(Ω.).*

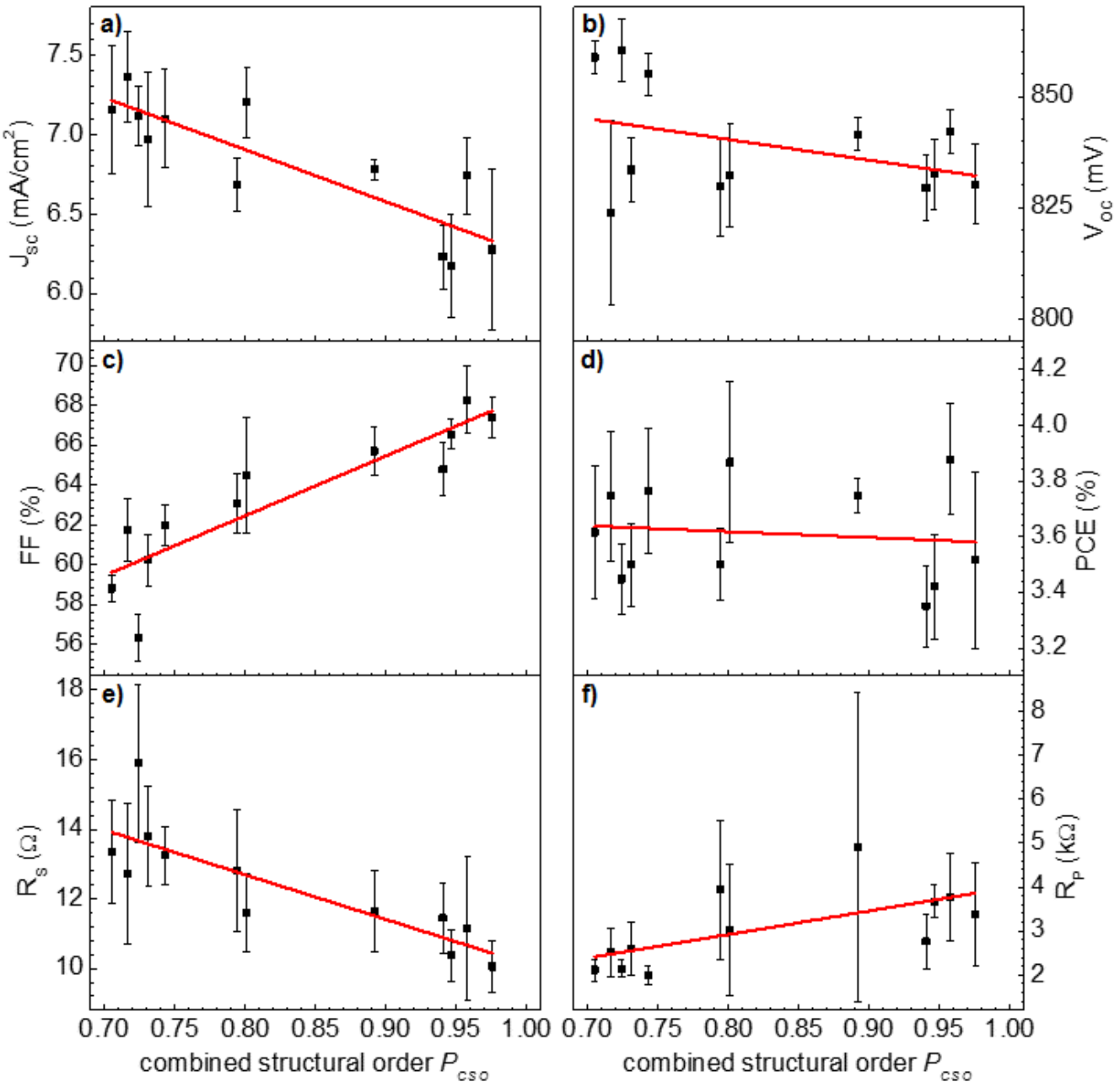

Figure 10: All photovoltaic parameters (a) J_{SC}, b) V_{OC}, c) *FF*, d) *PCE*, e) R_S, and f) R_P) replotted as function of the combined structural order parameter P_{CSO}. The black squares correspond to the mean-value of all solar cells investigated, whereas the standard deviation is depicted as range. The red line is a linear fit to the statistical data with respect to the P_{CSO}.

Conclusion

The aggregation of the semi-crystalline polymer AnE-PV*stat* was controlled in polymer-fullerene bulk heterojunction blends with PCBM by variation of the processing parameters polymer solution concentration and PCBM content. The optical analysis via absorption and photoluminescence spectroscopy revealed that AnE-PV*stat* is forming J-aggregates. Whereas the 0-0 to 0-1 peak ratio in

absorption indicated the extent of inter-chain order, respectively π–π stacking, the 0-0 to 0-1 peak ratio of the photoluminescence provided information about the intra-chain order, respectively planarity of the polymer. In our semi-quantitative approach we normalized these peak ratios to the obtained maximum and unified both into a single combined structural order parameter P_{CSO}. By analyzing and relating all photovoltaic parameters to the combined structural order, we find convincing evidence, that polymer aggregation

- supports charge extraction – as confirmed by increased fill factor and reduced series resistance,
- reduces photocurrent generation – presumably due to reduction in interfacial area, and
- slightly reduces photovoltage – pointing out that aggregation yields energetic relaxation.

Overall the variation in polymer aggregation did not have any remarkable impact on the power conversion efficiency, as the above mentioned effect were balanced out, which indicates the present material system to be optimized at its maximum performance within the parameter range studied. In conclusion, by the model material system applied in this study, a number of hypotheses concerning the effect of subtle morphological changes in terms of phase separation and domain ordering, could be verified. Future studies will be focused on precisely quantifying the extent of phase separation, the volume fraction of ordered polymer phases and the exciton and charge carrier dynamics.

Acknowledgements

The authors are grateful for financial support by DFG within the framework of SPP 1355. C.K. is grateful to the ***Thüringer Landesgraduiertenschule für Photovoltaik*** (PhotoGrad) for financial support.

References

1. A. J. Heeger, *Advanced Materials*, 2014, **26**, 10-28.
2. P. Kumar and S. Chand, *Progress in Photovoltaics*, 2012, **20**, 377-415.
3. G. Li, R. Zhu and Y. Yang, *Nature Photonics*, 2012, **6**, 153-161.
4. W. Yanmin, *Journal of Solar Energy Engineering*, 2012, **134**, 011017 (011019 pp.)-011017 (011019 pp.).
5. T. T. Larsen-Olsen, F. Machui, B. Lechene, S. Berny, D. Angmo, R. Soslashndergaard, N. Blouin, W. Mitchell, S. Tierney, T. Cull, P. Tiwana, F. Meyer, M. Carrasco-Orozco, A. Scheel, W. Loumlvenich, R. de Bettignies, C. J. Brabec and F. C. Krebs, *Adv. Energy Mater.*, 2012, **2**, 1091-1094.
6. F. C. Krebs, S. A. Gevorgyan and J. Alstrup, *J. Mater. Chem.*, 2009, **19**, 5442-5451.
7. F. C. Krebs, M. Jorgensen, K. Norrman, O. Hagemann, J. Alstrup, T. D. Nielsen, J. Fyenbo, K. Larsen and J. Kristensen, *Sol. Energy Mater. Sol. Cells*, 2009, **93**, 422-441.
8. G. M. Ng, E. L. Kietzke, T. Kietzke, L. W. Tan, P. K. Liew and F. R. Zhu, *Appl. Phys. Lett.*, 2007, **90**.
9. T. Ameri, G. Dennler, C. Waldauf, H. Azimi, A. Seemann, K. Forberich, J. Hauch, M. Scharber, K. Hingerl and C. J. Brabec, *Adv. Funct. Mater.*, 2010, **20**, 1592-1598.

10. D. Han, H. Kim, S. Lee, M. Seo and S. Yoo, *Optics Express*, 2010, **18**, A513-A521.
11. S. E. Shaheen, D. S. Ginley and G. E. Jabbour, *Mrs Bulletin*, 2005, **30**, 10-19.
12. E. Ahlswede, W. Muhleisen, M. W. B. M. Wahi, J. Hanisch and M. Powalla, *Appl. Phys. Lett.*, 2008, **92**.
13. S.-I. Na, B.-K. Yu, S.-S. Kim, D. Vak, T.-S. Kim, J.-S. Yeo and D.-Y. Kim, *Sol. Energy Mater. Sol. Cells*, 2010, **94**, 1333-1337.
14. N. S. Sariciftci, L. Smilowitz, A. J. Heeger and F. Wudl, *Synthetic Metals*, 1993, **59**, 333-352.
15. G. Yu, J. Gao, J. C. Hummelen, F. Wudl and A. J. Heeger, *Science*, 1995, **270**, 1789-1791.
16. N. S. Sariciftci, L. Smilowitz, A. J. Heeger and F. Wudl, *Science*, 1992, **258**, 1474-1476.
17. B. Kraabel, C. H. Lee, D. McBranch, D. Moses, N. S. Sariciftci and A. J. Heeger, *Chemical Physics Letters*, 1993, **213**, 389-394.
18. R. A. J. Janssen, J. C. Hummelen, K. Lee, K. Pakbaz, N. S. Sariciftci, A. J. Heeger and F. Wudl, *Journal of Chemical Physics*, 1995, **103**, 788-793.
19. Y. He and Y. Li, *Physical chemistry chemical physics : PCCP*, 2011, **13**, 1970-1983.
20. B. M. Savoie, A. Rao, A. A. Bakulin, S. Gelinas, B. Movaghar, R. H. Friend, T. J. Marks and M. A. Ratner, *J. Am. Chem. Soc.*, 2014, **136**, 2876-2884.
21. A. Pivrikas, N. S. Sariciftci, G. Juška and R. Österbacka, *Progress in Photovoltaics: Research and Applications*, 2007, **15**, 677-696.
22. M. T. Dang, L. Hirsch, G. Wantz and J. D. Wuest, *Chemical Reviews*, 2013.
23. C. R. Singh, G. Gupta, R. Lohwasser, S. Engmann, J. Balko, M. Thelakkat, T. Thurn-Albrecht and H. Hoppe, *Journal of Polymer Science Part B-Polymer Physics*, 2013, **51**, 943-951.
24. D. T. Duong, V. Ho, Z. Shang, S. Mollinger, S. C. B. Mannsfeld, J. Dacuña, M. F. Toney, R. Segalman and A. Salleo, *Adv. Funct. Mater.*, 2014, n/a-n/a.
25. S. Rathgeber, D. B. de Toledo, E. Birckner, H. Hoppe and D. A. M. Egbe, *Macromolecules*, 2010, **43**, 306-315.
26. S. Rathgeber, J. Perlich, F. Kuhnlenz, S. Turk, D. A. M. Egbe, H. Hoppe and R. Gehrke, *Polymer*, 2011, **52**, 3819-3826.
27. E. J. W. Crossland, K. Tremel, F. Fischer, K. Rahimi, G. Reiter, U. Steiner and S. Ludwigs, *Advanced Materials*, 2012, **24**, 839-+.
28. R. Noriega, J. Rivnay, K. Vandewal, F. P. V. Koch, N. Stingelin, P. Smith, M. F. Toney and A. Salleo, *Nature Mater.*, 2013, **12**, 1037-1043.
29. C. Kästner, X. Jiao, D. A. M. Egbe, H. W. Ade and H. Hoppe, *Proc. SPIE 9184*, 2014, **Organic Photovoltaics XV**.
30. C. Waldauf, P. Schilinsky, M. Perisutti, J. Hauch and C. J. Brabec, *Advanced Materials*, 2003, **15**, 2084-2088.
31. T. B. Singh, N. Marjanović, G. J. Matt, S. Günes, N. S. Sariciftci, A. Montaigne Ramil, A. Andreev, H. Sitter, R. Schwödiauer and S. Bauer, *Organic Electronics*, 2005, **6**, 105-110.
32. S. Gelinas, A. Rao, A. Kumar, S. L. Smith, A. W. Chin, J. Clark, T. S. van der Poll, G. C. Bazan and R. H. Friend, *Science*, 2014, **343**, 512-516.
33. F. C. Jamieson, E. B. Domingo, T. McCarthy-Ward, M. Heeney, N. Stingelin and J. R. Durrant, *Chemical Science*, 2012, **3**, 485-492.
34. S. M. Menke and R. J. Holmes, *Energy & Environmental Science*, 2014.
35. I. W. Hwang, D. Moses and A. J. Heeger, *Journal of Physical Chemistry C*, 2008, **112**, 4350-4354.
36. J. Nelson, *Materials Today*, 2011, **14**, 462-470.
37. M. A. Brady, G. M. Su and M. L. Chabinyc, *Soft Matter*, 2011, **7**, 11065-11077.
38. F. Liu, Y. Gu, J. W. Jung, W. H. Jo and T. P. Russell, *Journal of Polymer Science Part B: Polymer Physics*, 2012, **50**, 1018-1044.
39. N. D. Treat and M. L. Chabinyc, *Annual Review of Physical Chemistry*, 2014, **65**, 59-81.
40. S.-S. Sun, *Sol. Energy Mater. Sol. Cells*, 2003, **79**, 257-264.

41. S. M. Lindner and M. Thelakkat, *Macromolecules*, 2004, **37**, 8832-8835.
42. F. Padinger, R. S. Rittberger and N. S. Sariciftci, *Adv. Funct. Mater.*, 2003, **13**, 85-88.
43. W. L. Ma, C. Y. Yang, X. Gong, K. Lee and A. J. Heeger, *Adv. Funct. Mater.*, 2005, **15**, 1617-1622.
44. G. Li, V. Shrotriya, J. S. Huang, Y. Yao, T. Moriarty, K. Emery and Y. Yang, *Nature Mater.*, 2005, **4**, 864-868.
45. X. N. Yang, J. Loos, S. C. Veenstra, W. J. H. Verhees, M. M. Wienk, J. M. Kroon, M. A. J. Michels and R. A. J. Janssen, *Nano Letters*, 2005, **5**, 579-583.
46. N. Kiriy, E. Jahne, H. J. Adler, M. Schneider, A. Kiriy, G. Gorodyska, S. Minko, D. Jehnichen, P. Simon, A. A. Fokin and M. Stamm, *Nano Lett.*, 2003, **3**, 707-712.
47. W. Y. Huang, P. T. Huang, Y. K. Han, C. C. Lee, T. L. Hsieh and M. Y. Chang, *Macromolecules*, 2008, **41**, 7485-7489.
48. A. J. Moule and K. Meerholz, *Advanced Materials*, 2008, **20**, 240-+.
49. S. Y. Sun, T. Salim, L. H. Wong, Y. L. Foo, F. Boey and Y. M. Lam, *J. Mater. Chem.*, 2011, **21**, 377-386.
50. M. J. Sobkowicz, R. L. Jones, R. J. Kline and D. M. DeLongchamp, *Macromolecules*, 2012, **45**, 1046-1055.
51. H. Yan, Y. Yan, Z. Yu and Z. Wei, *Journal of Physical Chemistry C*, 2011, **115**, 3257-3262.
52. K. Vakhshouri, D. R. Kozub, C. Wang, A. Salleo and E. D. Gomez, *Phys Rev Lett*, 2012, **108**, 026601.
53. F. C. Chen, H. C. Tseng and C. J. Ko, *Appl. Phys. Lett.*, 2008, **92**, 3.
54. J. K. Lee, W. L. Ma, C. J. Brabec, J. Yuen, J. S. Moon, J. Y. Kim, K. Lee, G. C. Bazan and A. J. Heeger, *Journal of the American Chemical Society*, 2008, **130**, 3619-3623.
55. Y. Yao, J. Hou, Z. Xu, G. Li and Y. Yang, *Adv. Funct. Mater.*, 2008, **18**, 1783-1789.
56. H. Sirringhaus, P. J. Brown, R. H. Friend, M. M. Nielsen, K. Bechgaard, B. M. W. Langeveld-Voss, A. J. H. Spiering, R. A. J. Janssen, E. W. Meijer, P. Herwig and D. M. de Leeuw, *Nature*, 1999, **401**, 685-688.
57. H. Hoppe, T. Glatzel, M. Niggemann, W. Schwinger, F. Schaeffler, A. Hinsch, M. C. Lux-Steiner and N. S. Sariciftci, *Thin Solid Films*, 2006, **511–512**, 587-592.
58. N. C. Cates, R. Gysel, J. E. P. Dahl, A. Sellinger and M. D. McGehee, *Chem. Mat.*, 2010, **22**, 3543-3548.
59. D. A. M. Egbe, S. Turk, S. Rathgeber, F. Kuhnlenz, R. Jadhav, A. Wild, E. Birckner, G. Adam, A. Pivrikas, V. Cimrova, G. Knor, N. S. Sariciftci and H. Hoppe, *Macromolecules*, 2010, **43**, 1261-1269.
60. C. Kastner, S. Rathgeber, D. A. M. Egbe and H. Hoppe, *Journal of Materials Chemistry A*, 2013, **1**, 3961-3969.
61. C. Kästner, B. Muhsin, A. Wild, D. A. M. Egbe, S. Rathgeber and H. Hoppe, *J. Polym. Sci. Part B: Polym. Phys.*, 2013, **10.1002/polb.23286**.
62. J. Clark, J. F. Chang, F. C. Spano, R. H. Friend and C. Silva, *Applied Physics Letters*, 2009, **94**.
63. H. Yamagata and F. C. Spano, *Journal of Chemical Physics*, 2012, **137**.
64. F. C. Spano, J. Clark, C. Silva and R. H. Friend, *Journal of Chemical Physics*, 2009, **130**.
65. R. Osterbacka, C. P. An, X. M. Jiang and Z. V. Vardeny, *Science*, 2000, **287**, 839-842.
66. S. R. Amrutha and M. Jayakannan, *The journal of physical chemistry. B*, 2008, **112**, 1119-1129.
67. D. Baeriswyl, D. Campbell and S. Mazumdar, in *Conjugated Conducting Polymers*, ed. H. Kiess, Springer Berlin Heidelberg, 1992, pp. 7-133.
68. K. Pichler, D. A. Halliday, D. D. C. Bradley, P. L. Burn, R. H. Friend and A. B. Holmes, *Journal of Physics-Condensed Matter*, 1993, **5**, 7155-7172.
69. R. Hoofman, M. P. de Haas, L. D. A. Siebbeles and J. M. Warman, *Nature*, 1998, **392**, 54-56.
70. B. J. Schwartz, T. Q. Nguyen, J. J. Wu and S. H. Tolbert, *Synthetic Metals*, 2001, **116**, 35-40.

71. H. Hoppe, M. Niggemann, C. Winder, J. Kraut, R. Hiesgen, A. Hinsch, D. Meissner and N. S. Sariciftci, *Adv. Funct. Mater.*, 2004, **14**, 1005-1011.
72. P. J. Flory, *Journal of Chemical Physics*, 1945, **13**, 453-465.
73. C. Kästner, D. K. Susarova, R. Jadhav, C. Ulbricht, D. A. M. Egbe, S. Rathgeber, P. A. Troshin and H. Hoppe, *J. Mater. Chem.*, 2012, **22**, 15987.
74. M. Hallermann, I. Kriegel, E. Da Como, J. M. Berger, E. von Hauff and J. Feldmann, *Adv. Funct. Mater.*, 2009, **19**, 3662-3668.
75. P. J. Flory, *The Journal of Chemical Physics*, 1945, **13**, 453-465.
76. N. C. Cates, R. Gysel, Z. Beiley, C. E. Miller, M. F. Toney, M. Heeney, I. McCulloch and M. D. McGehee, *Nano Lett*, 2009, **9**, 4153-4157.
77. N. C. Miller, E. Cho, M. J. N. Junk, R. Gysel, C. Risko, D. Kim, S. Sweetnam, C. E. Miller, L. J. Richter, R. J. Kline, M. Heeney, I. McCulloch, A. Amassian, D. Acevedo-Feliz, C. Knox, M. R. Hansen, D. Dudenko, B. F. Chmelka, M. F. Toney, J.-L. Brédas and M. D. McGehee, *Advanced Materials*, 2012, **24**, 6071-6079.
78. N. C. Miller, E. Cho, R. Gysel, C. Risko, V. Coropceanu, C. E. Miller, S. Sweetnam, A. Sellinger, M. Heeney, I. McCulloch, J.-L. Brédas, M. F. Toney and M. D. McGehee, *Advanced Energy Materials*, 2012, **2**, 1208-1217.
79. R. Koeppe and N. S. Sariciftci, *Photochem. Photobiol. Sci.*, 2006, **5**, 1122-1131.
80. C. Kastner, C. Ulbricht, D. A. M. Egbe and H. Hoppe, *Journal of Polymer Science Part B-Polymer Physics*, 2012, **50**, 1562-1566.
81. A. Viterisi, F. Gispert-Guirado, J. W. Ryan and E. Palomares, *J. Mater. Chem.*, 2012, **22**, 15175-15182.
82. Y. Kim, S. Cook, S. M. Tuladhar, S. A. Choulis, J. Nelson, J. R. Durrant, D. D. C. Bradley, M. Giles, I. McCulloch, C. S. Ha and M. Ree, *Nature Mater.*, 2006, **5**, 197-203.
83. T. M. Clarke, A. M. Ballantyne, J. Nelson, D. D. C. Bradley and J. R. Durrant, *Adv. Funct. Mater.*, 2008, **18**, 4029-4035.

Polymer Aggregation Control in Polymer:Fullerene Bulk Heterojunctions Adapted from Solution

Christian Kästner, Daniel A. M. Egbe, Harald Hoppe

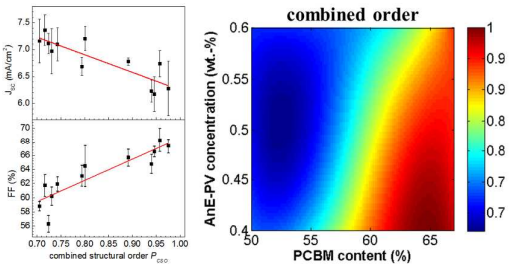

In a semi-quantitative approach, we unified inter-chain and intra-chain polymer order into a single parameter of combined structural order P_{CSO}. Relating all photovoltaic parameters to the P_{CSO}, we find convincing evidence, that polymer aggregation supports charge extraction, reduces photocurrent generation and slightly reduces photovoltage.